Supporting Information

Critical Role of Interfacial Effects on the Reactivity of Semiconductor-Cocatalyst Junctions for Photocatalytic Oxygen Evolution from Water

John C. Matsubu[‡†], *Eric T. Lin*[‡†], *Kyle L. Gunther*[†], *Krassimir N. Bozhilov*[⊥], *Yibo Jiang*[†], *Phillip Christopher*[†,#,§,*]

[†]Department of Chemical & Environmental Engineering, University of California, Riverside, Riverside, California 92521, United States

[⊥]Central Facility for Advanced Microscopy and Microanalysis, University of California, Riverside, California 92521

[#]Program in Materials Science, University of California, Riverside, Riverside, CA 92521, USA.

[§]UCR Center for Catalysis, University of California, Riverside, Riverside, CA 92521, USA.

*Corresponding Author E-mail: christopher@engr.ucr.edu

Contents

Figure S8: HAADF STEM-CoO_x/ZnO

Figure S9: HAADF STEM-CoO_x/SnO_2

Figure S10: Weight loading depe ndent OER rates for CCs on ZnO

Table S1. Temperature and duration of sample calcination in air during CC synthesis on the SCs.

Co-Catalyst	Temperature (˚C)	Hours
IrO_x	550	5
MnO_x	400	2
RuO_x	400	6
NiO_x	400	3
CoO_x	500	2

Table S2. SC Crystal structures and lattice parameters determined from XRD

	$BiVO_4$	ZnO	SnO_2
Crystal Structure	Monoclinic	Wurtzite (hexagonal)	Rutile (Tetragonal)
Lattice Constant A	5.19	3.25	4.72
Lattice Constant B	5.09	-	-
Lattice Constant C	11.70	5.20	3.19

Table S3. CC crystal structures and lattice parameters of SC and CC determined from previous studies.

	RuO_2	IrO_2	MnO_2	Co_3O_4	NiO
Crystal Structure[1]	Rutile	Rutile	Rutile	Spinel	Rock Salt
Lattice Constant A[1,2]	4.50	4.51	4.40	8.08	4.18
Lattice Constant C[1,2]	3.10	3.16	2.87	-	-
Conduction Type[1]	Metallic	Metallic	Semi	Semi	Semi

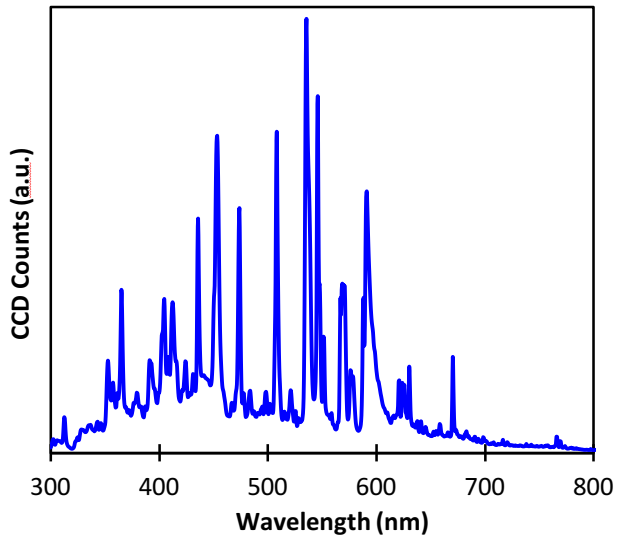

Figure S1. Spectral output of metal halide lamp (MH100A)

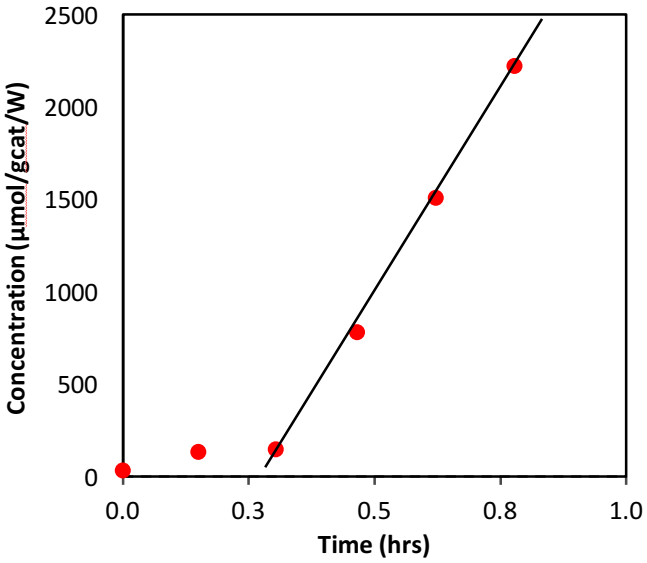

Figure S2. Typical O_2 accumulation plot, where slope of accumulation at onset of reactor illumination was used to determine OER rate.

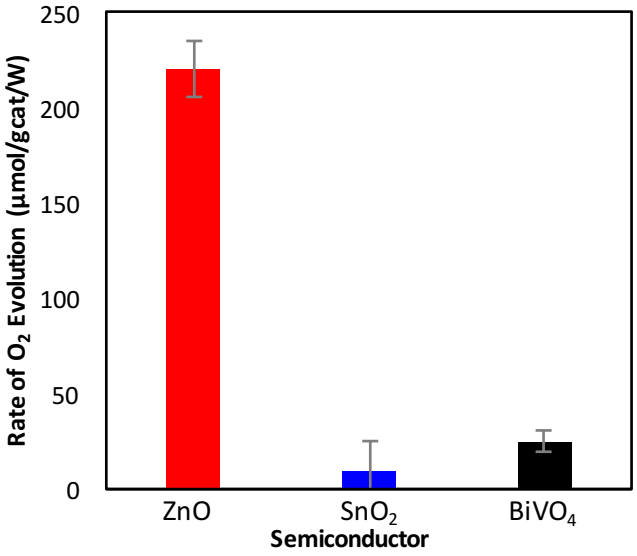

Figure S3. Rate of OER rate normalized per gram catalyst and power of lamp for ZnO, SnO_2, and $BiVO_4$ SCs. The rates for each SC were determined from the slope of the O_2 accumulation vs time plots similar to fig S2. Error bars were determined from testing the performance of each catalyst sample twice.

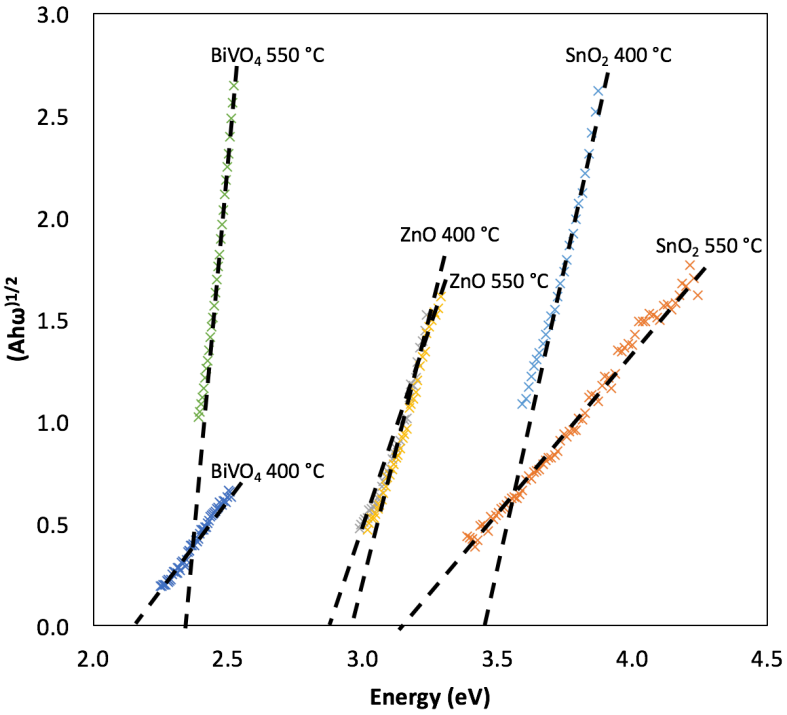

Fig S4. Plot of Kubelka-Munk function used to calculate band gap energies for SC pretreated at different conditions during CC synthesis.

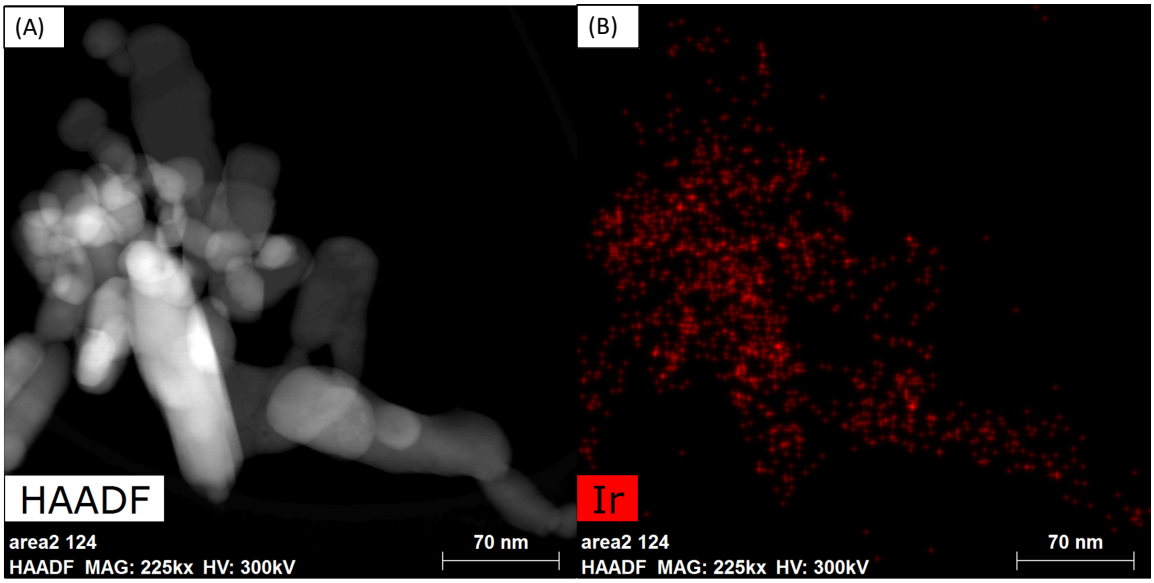

Figure S5. (A) HAADF STEM analysis of 1% IrO_x/ZnO. (B) Corresponding EDS map showing high IrO_x dispersion with particle sizes < 5nm.

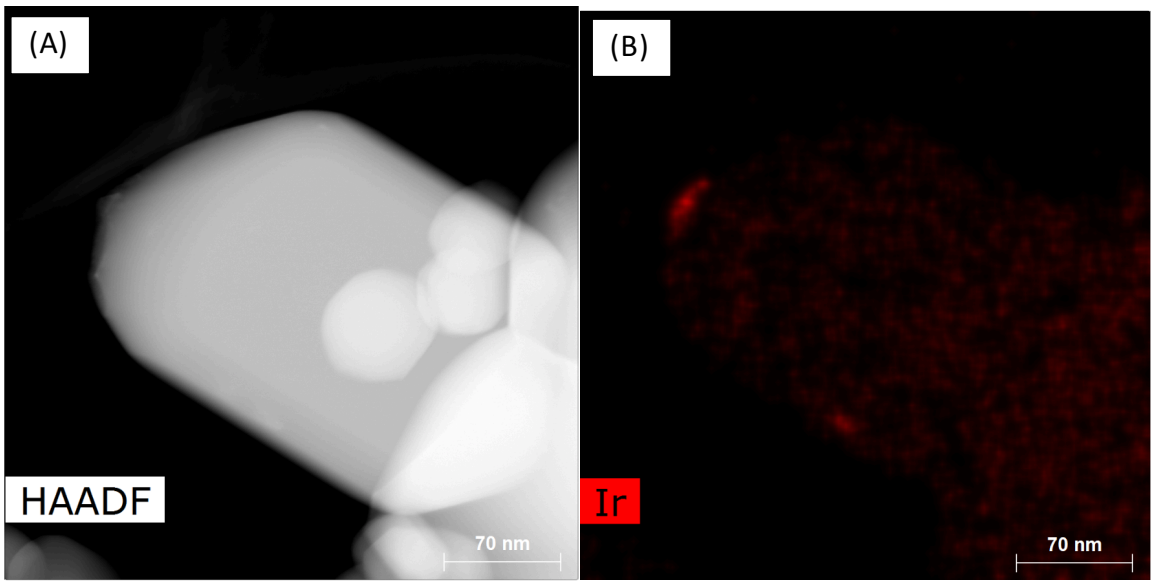

Figure S6. (A) HAADF STEM analysis of 1% IrO_x/SnO_2. (B) Corresponding EDS map showing high IrO_x dispersion with particle sizes < 5nm.

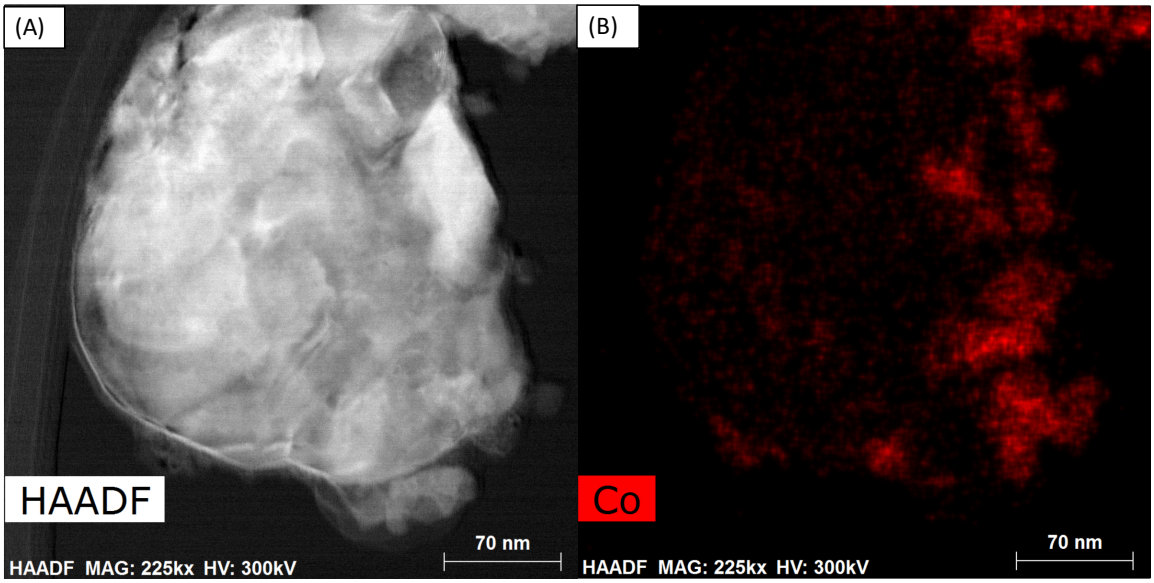

Figure S7. (A) HAADF STEM analysis of 1% $CoO_x/BiVO_4$. (B) Corresponding EDS map indicating Co NPs were present on the SC surface with particle and/or particle aggregations with sizes from <5nm up to 70nm.

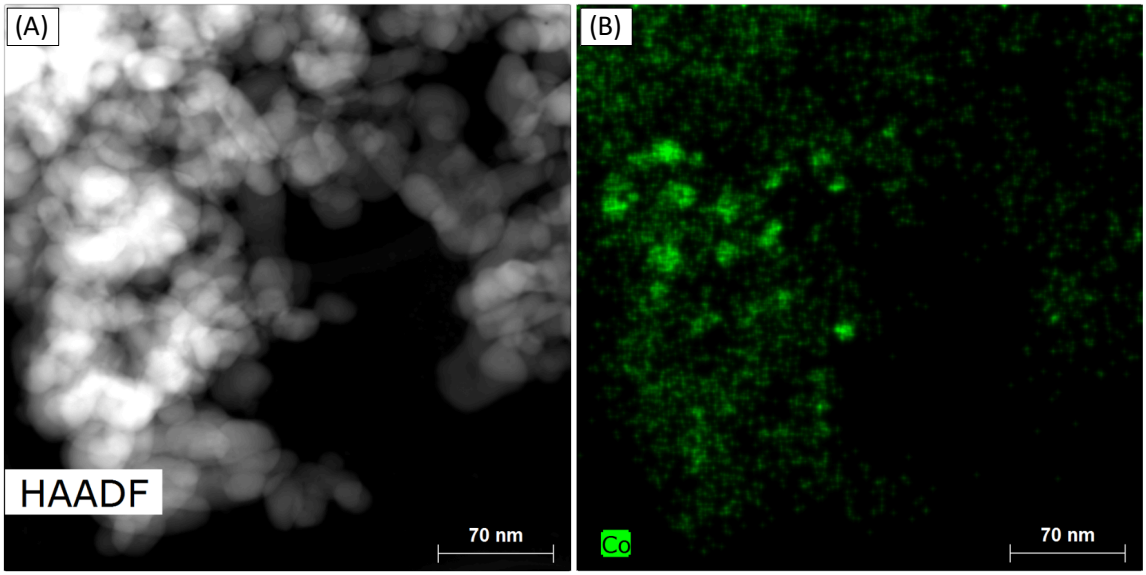

Figure S8. (A) HAADF STEM analysis of 1% CoO_x/ZnO. (B) Corresponding EDS map indicating Co NPs were present on the SC surface with particle and/or particle aggregations with sizes from <2nm up to ~20nm.

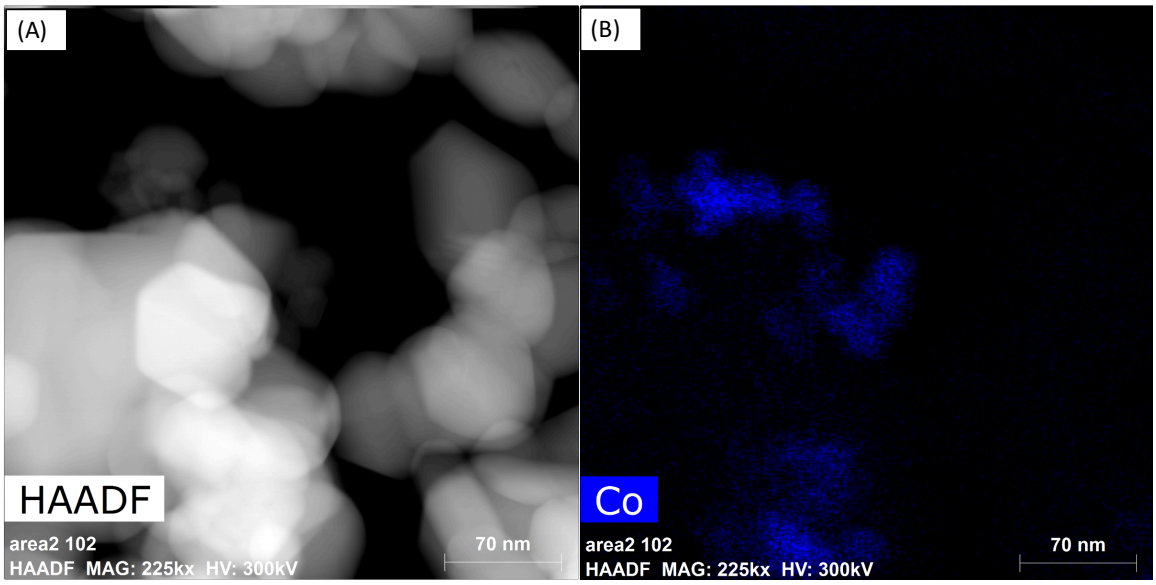

Figure S9. (A) HAADF STEM analysis of 1% CoO_x/SnO_2. (B) Corresponding EDS map showing CoO_x formed large NPs or aggregates on SnO_2 of 15-70nm.

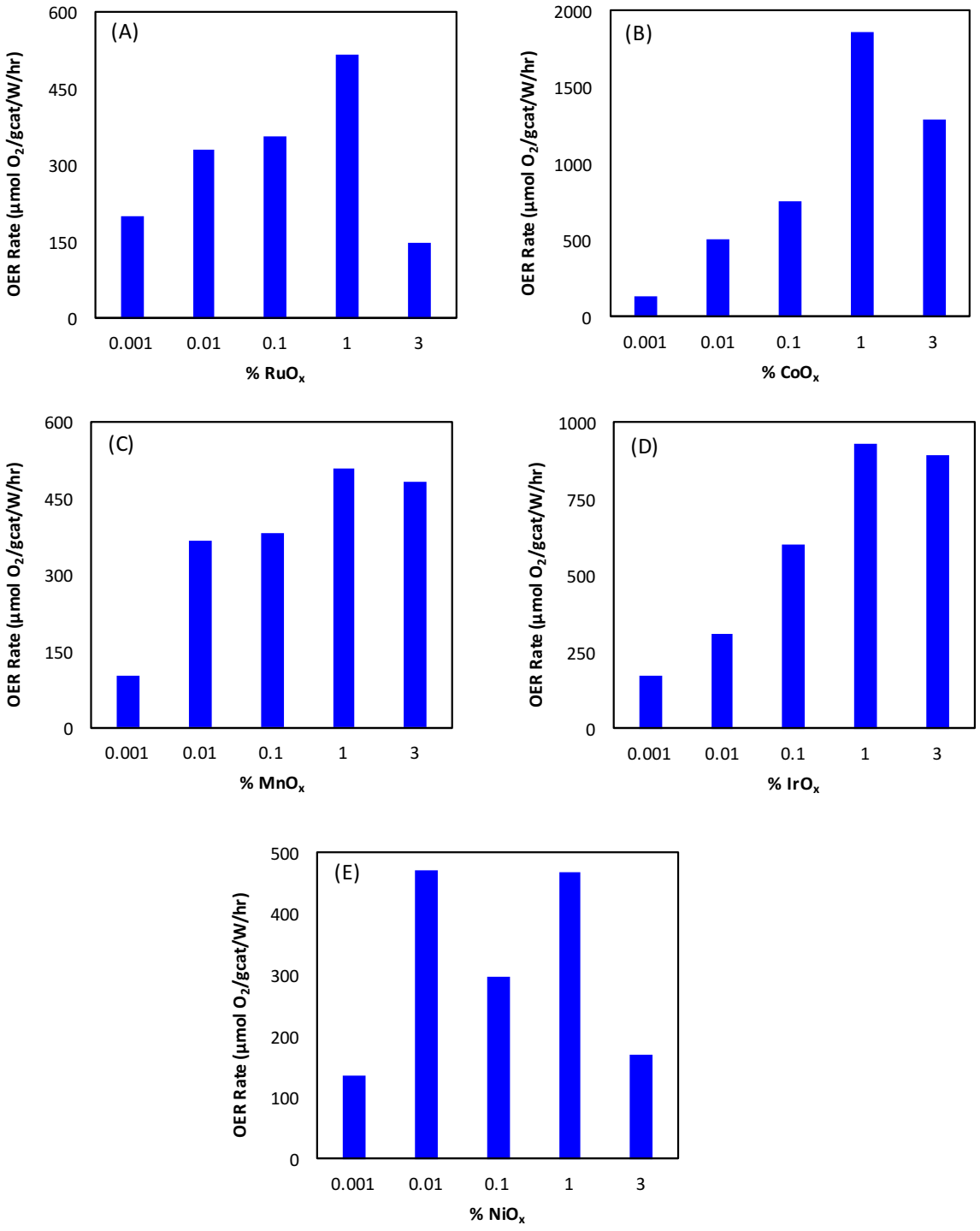

Figure S10. OER rates for varying CC weight loadings on ZnO SC with CCs: (A) RuO_x, (B) CoO_x, (C) MnO_x, (D) IrO_x and, (E) NiO_x

These samples were illuminated with 365nm light causing the rate per watt of illumination ~3-fold larger than the OER rates in Fig. 3.

References

1. A. Bolzan, C. Fong, B. J. Kennedy and C. J. Howard, *Acta Crystallogr. Sect. B*, 1997, **B53**, 373–380.

2. N. R. Rao and G.V. Subba Rao, *Transition Metal Oxides: Crystal Chemistry, Phase Transition, and Related Aspects*; U.S. Govt. Print. Off: Washington., 1974.